ADVANCED OPTICAL MATERIALS
www.advopticalmat.de

Programmable Coloration and Patterning on Reconfigurable Chiral Photonic Paper

*Shuzhen Cui, Lang Qin, Xiaojun Liu, and Yanlei Yu**

Responsive photonic crystals are widely employed to construct rewritable paper, where patterns are written and erased repeatedly via color switching. The working principle mainly lies in the changes on the lattice constant of periodic structures, which, however, restricts the localized color tuning of the recorded patterns and thus limits multicolor information transfer. Herein, a novel strategy is reported to write, erase, and importantly to tune the colors by developing unique light-driven cholesteric liquid crystals (CLCs) that possess self-organized helical superstructures with two structural elements of pitch lengths (lattice constant) and helical axes (reconfiguration). Reconfiguration of the helical axes provides two high-contrast optical states for writing and erasing by pressure and electricity, whereas precise photocontrol of the pitch lengths contributes to localized color tuning. These features primarily capitalize on the light-driven CLC with diverse photostationary colors, which is induced by a newly designed binary chiral system and confined in the polymer dispersed liquid crystal layer. Distinct multicolor patterns are mechanically written, optically tuned, and electrically erased on the rewritable photonic paper in a programmable manner. Such photonic paper has potential to record, program, and remember optically addressed images in visualized color information and user-interactive display technologies.

1. Introduction

Rewritable paper, performing "write–erase" cycles repeatedly via color switching, is a potential alternative to conventional paper, which helps to alleviate global deforestation mainly caused by the increasing paper consumption.[1] Such rewritability highly capitalizes on chromogenic materials that undergo reversible color switching promoted by external stimulation.[2–7] As one of the chromogenic materials, responsive photonic crystals, composed of the periodically structured materials with different refractive indices, exhibit tunable structural colors[8–12] and thus have been investigated advantageously in creating the rewritable photonic paper.[13–18] Hitherto, researchers strive to develop different rewritable paper by using responsive photonic crystals, where the periodic structures are closely related to the features of the used materials. For example, opal structures are constructed by embedding colloidal nanoparticles (e.g., silica, Fe_3O_4, and polystyrene microbeads) into smart polymer matrices.[19–22] Lamellar structures are fabricated by self-assembly of block copolymers or layer-by-layer deposition of metals and their oxides.[23–25] In these photonic paper, the working principle behind the process of writing and erasing mainly lies in the changes on the lattice constant of periodic structures, which, however, restricts localized color tuning of the recorded patterns and consequently limits accurate transfer of intricate multicolor information. Therefore, an alternative working principle of writing, erasing, and tuning is needed to be developed for the responsive photonic crystals.

To address the challenge, we propose a novel strategy to write, erase, and notably to tune the structural colors by manipulating both the lattice constant and reconfiguration of the photonic structures; the changes on the lattice are independently responsible for tuning of the structural colors, while the reconfigurability between periodic and disordered architectures provides two optical states for writing and erasing. An ideal candidate compatible with this new working principle is the light-driven cholesteric liquid crystal (CLC), which is a kind of unique soft photonic crystals and possesses two key structural elements, i.e., phototunable pitch length (for tuning) and reconfigurable helical axis (for writing and erasing).[26,27]

The light-driven CLCs facilitate localized color tuning because light, compared to other stimuli, has spatial superiority of remote and local control.[28] The pitch length that determines the reflection wavelength according to Bragg's law can be manipulated by light stimuli due to the photoresponsive chiral switches doped in the CLCs.[29,30] The chiral switches twist the liquid crystal (LC) molecules into helical superstructures[31,32] and undergo configurational changes upon photoisomerization, leading to variation in the helical twisting power (HTP, β), the pitch length, and consequently the structural colors (tuning).[33–35] Currently, chiral switches based on azobenzene have been extensively studied as they have large variation in the HTP values, and enable a wide tuning range of the resultant CLCs to cover entire visible spectrum.[36–38] Furthermore, the alignment of the helical axes in CLCs offers

S. Cui, L. Qin, X. Liu, Y. Yu
Department of Materials Science & State Key Laboratory of Molecular Engineering of Polymers
Fudan University
Shanghai 200433, P. R. China
E-mail: ylyu@fudan.edu.cn
The ORCID identification number(s) for the author(s) of this article can be found under https://doi.org/10.1002/adom.202102108.

DOI: 10.1002/adom.202102108

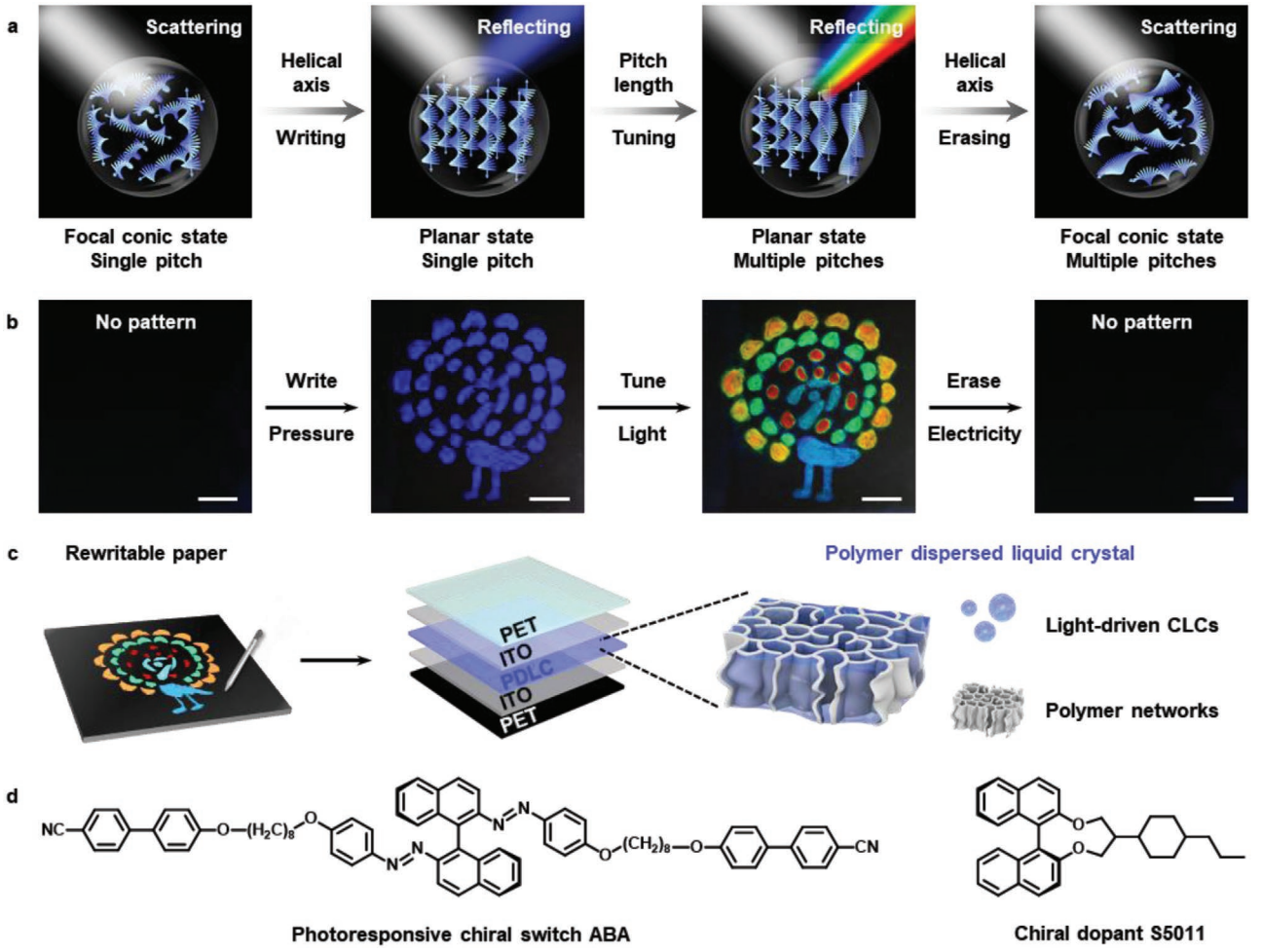

Figure 1. a) Schematic illustration to show the working principle of the rewritable photonic paper capitalizing on the reconfigurable helical axis and phototunable pitch length in light-driven cholesteric liquid crystals (CLCs). Writing is the reconfiguration of the helical axes from focal conic (FC) state to planar state. Tuning is the manipulation of the pitch lengths. Erasing is the switching of the helical axes from planar state to FC state. b) Photographs of the resultant photonic paper to show the writing, tuning, and erasing of a multicolor pattern. The blue "peacock" is clearly written upon pressure, locally tuned to colorful "peacock" by light of different wavelengths, and completely erased with the application of an electric field. Scale bar, 1 cm. c) Schematic illustration to show the internal structures of the photonic paper. The polymer dispersed liquid crystal (PDLC) composed of light-driven CLCs and polymer networks is sandwiched between transparent and black PET films with indium–tin oxide (ITO) electrodes. d) Chemical structures of the binary chiral system used to prepare the light-driven CLCs in the LC host E7, including photoresponsive chiral switch ABA and chiral dopant S5011.

two optical states with high-contrast colors, including reflecting planar state and scattering focal conic (FC) state. Switching of the helical axes between orderly oriented planar state and randomly aligned FC state can be employed for the "write–erase" cycles (writing and erasing).[39,40] However, the light-driven CLCs, while promising, suffer from limitations that restrict their applicability in the construction of the rewritable paper. First, the phototunable structural colors are predominately unstable at the transition states, unlike photostationary states (PSSs),[41] which strongly impacts the accurate record of multicolor information. Moreover, the pure CLC mixtures are prone to blurry handwriting even under local stress, arising from the fluidity and cooperative effect of the LCs.[42]

Herein, rewritable photonic paper capable of writing, erasing, and especially localized color tuning is designed by combining the reconfigurable helical axis and phototunable pitch length in self-organized helical superstructures (**Figure 1**a). For example, a blue "peacock" is written on the rewritable paper by pressure, then "spreads its colorful tail" after localized phototuning of the structural colors, and is completely erased with the application of an electric field (Figure 1b; Movie S1, Supporting Information). Such functions are primarily ascribed to the internal polymer dispersed liquid crystal (PDLC) layer composed of the light-driven CLCs and polymer networks, which provide photostationary colors and sharp outlines for recorded patterns, respectively (Figure 1c). One should be emphasized that the basic "write–erase" cycles are upgraded to novel "write–tune–erase" and "tune–write–erase" modes based on orthogonal manipulation of the two structural elements (helical axis and pitch). We demonstrate the potential of our photonic paper to record, program, and remember intricate multicolor information in user-interactive display technology.

2. Results and Discussion

The rewritable photonic paper was designed based on three criteria: 1) the light-driven CLC must exhibit diverse photostationary colors; 2) the planar state must be locally reconfigured by pressure; and 3) the FC state must be stable even after the applied electric field is turned off. The first requirement is satisfied by doping a binary chiral system consisting of a photoresponsive chiral switch ABA and a chiral dopant S5011 into nematic LC host E7 (Figure 1d; see Figure S1 for synthetic routes in the Supporting Information). According to the empirical equation

$$\beta = c_1 \times \beta_1 + c_2 \times \beta_2 \quad (1)$$

the average HTP value of the binary chiral system (β) is determined by the concentration percentages (c_1, c_2) and the HTP values (β_1, β_2) of two chiral materials.[43] In this scenario, diverse photostationary colors of the light-driven CLCs are demonstrated thanks to the different and appropriate HTP values at each PSS induced by regulating both the photoisomerization of ABA and relative concentrations of two chiral materials. To satisfy the second and third requirements, polymers are introduced into the light-driven CLCs to form the PDLC, where the low-molecular-weight LCs are separated from the polymer networks during polymerization and are confined in microscale domains. The polymer networks preserve the LC orientation by anchoring effect, thus stabilizing the FC state at the zero electric field and also reducing the mobility of the LC molecules.[42,44] In light of these principles, we fabricated the photonic paper aiming at information transfer with diverse photostationary colors that can be locally tuned before and after writing.

It is important to note that the HTP values heavily rely on the chemical structures and configurations of the photoresponsive chiral switches, but are difficult to be precisely modulated to the appropriate values that enable the CLC at the PSSs to reflect light of different wavelengths in the visible spectrum.[26] Therefore, most of the existing light-driven CLCs containing only one photoresponsive chiral switch exhibited a few photostationary colors. Herein, the binary chiral system is constructed from newly synthetic ABA and commercially available S5011 to solve these problems. The binaphthalene moiety as an axially chiral center endows the chiral switch ABA with high HTP. The azobenzene photoswitches linked to the chiral center undergo reversible photoisomerization between rod-like *trans*-isomer and bent *cis*-isomer, leading to significant changes of the steric configurations of the (*trans*, *trans*) and (*cis*, *cis*) forms (**Figure 2**a). The flexible alkoxy groups ($-OC_8H_{17}O-$) together with the rigid core (4-cyanobiphenyl) are designed to mimic the structure of LC molecules and to increase the solubility of ABA in the LC host. As shown in Figure 2b, UV–vis spectra of ABA in CH_2Cl_2 solution were comprehensively investigated upon irradiation of 530, 470, 445, 365, and 405 nm light in sequence. The absorption intensity of the π–π^* band around 358 nm gradually decreases from the initial state to the PSS-405, indicating that the *trans*–*cis* photoisomerization of ABA with different photoconversion produces various isomer ratios of (*trans*, *trans*), (*trans*, *cis*), and (*cis*, *cis*) at the different PSSs.

By using wedge cells according to the Grandjean–Cano method (Figure S2, Supporting Information), we demonstrated that ABA shows an HTP value as high as 185 μm^{-1}, mol% (or 46 μm^{-1}, wt%) at the initial state (Figure S3, Supporting Information), which is larger than that of the previously reported photoresponsive chiral switch with a similar molecular structure (153 μm^{-1}, mol%).[36] This phenomenon is ascribed to the incorporation of the cyanobiphenyl groups that enhance the compatibility of ABA in the LC host E7, a eutectic mixture composed of several cyanobiphenyl derivatives. Moreover, the HTP value was modulated to 28, 26, 21, 3, and even 0 μm^{-1} (wt%) at the PSS-530, PSS-470, PSS-445, PSS-365, and PSS-405, respectively (Figure S3, Supporting Information), resulting from the configurational changes of ABA driven by light of different wavelengths (for convenience, the HTP values in the following text are calculated with mass fraction, wt%).

S5011 is chosen as the chiral dopant to prepare the binary chiral system with ABA because it shows a very high HTP value in the LC host E7 (111 μm^{-1}, wt%; Figure S4, Supporting Information), and meanwhile exhibits the same helicity as ABA, both of which twist the LC molecules into left-handed helical superstructures (Figure S5, Supporting Information). Considering the remarkably large variation in the HTP values between the initial state and PSS_{405} ($\Delta\beta/\beta_{ini}$ = 100%), we prepared a light-driven CLC by doping 3.5 wt% ABA and 2.2 wt% S5011 in the LC host E7, and demonstrated the dynamic phototuning of the selective reflection. The CLC mixture was filled into a 15 μm thick antiparallel aligned cell and reflected 410 nm light at the initial state. Upon exposure to light of different wavelengths within 30 s, the central reflection wavelength of the CLCs redshifted and was "fixed" at 485 nm (PSS-530), 500 nm (PSS-470), 528 nm (PSS-445), 610 nm (PSS-365), and 660 nm (PSS-405), respectively (Figure 2c), owing to the appropriate HTP values provided by the binary chiral system, where the experimental results (72, 62, 59, 55, 46, and 42 μm^{-1}, wt% at the different states) were consistent with the theoretical calculation (Figure 2d–i; Table S1, Supporting Information). Accordingly, the CLC mixture confined in the cell exhibits blue (410 nm), cyan (485 nm), turquoise (500 nm), green (528 nm), orange (610 nm), and red (660 nm) photostationary colors. It should be emphasized that a fixed relationship has been successfully established between the structural colors and light stimuli (Figures S6 and S7, Supporting Information), which is attributed to the constant HTP value of S5011 and exact HTP variation of ABA that possesses distinct equilibrium ratios of (*trans*, *trans*), (*trans*, *cis*), and (*cis*, *cis*) forms.[39] These results indicate that the light-driven CLCs induced by the binary chiral system are qualified as the responsive photonic crystals used to fabricate the photonic paper.

The local planar alignment and stable FC state are prerequisites for sharp handwriting and complete erasing. To this end, we introduce polymers into the light-driven CLCs to fabricate the PDLC via photopolymerization-induced phase separation,[45] which is sandwiched between two flexible polyethylene terephthalate (PET) substrates coated with indium–tin oxide (ITO) (**Figure 3**a). The upper transparent PET enables the propagation of the incident light, while the bottom black PET provides a contrast with the bright iridescent Bragg reflective colors. The detail of the fabrication procedure is described in

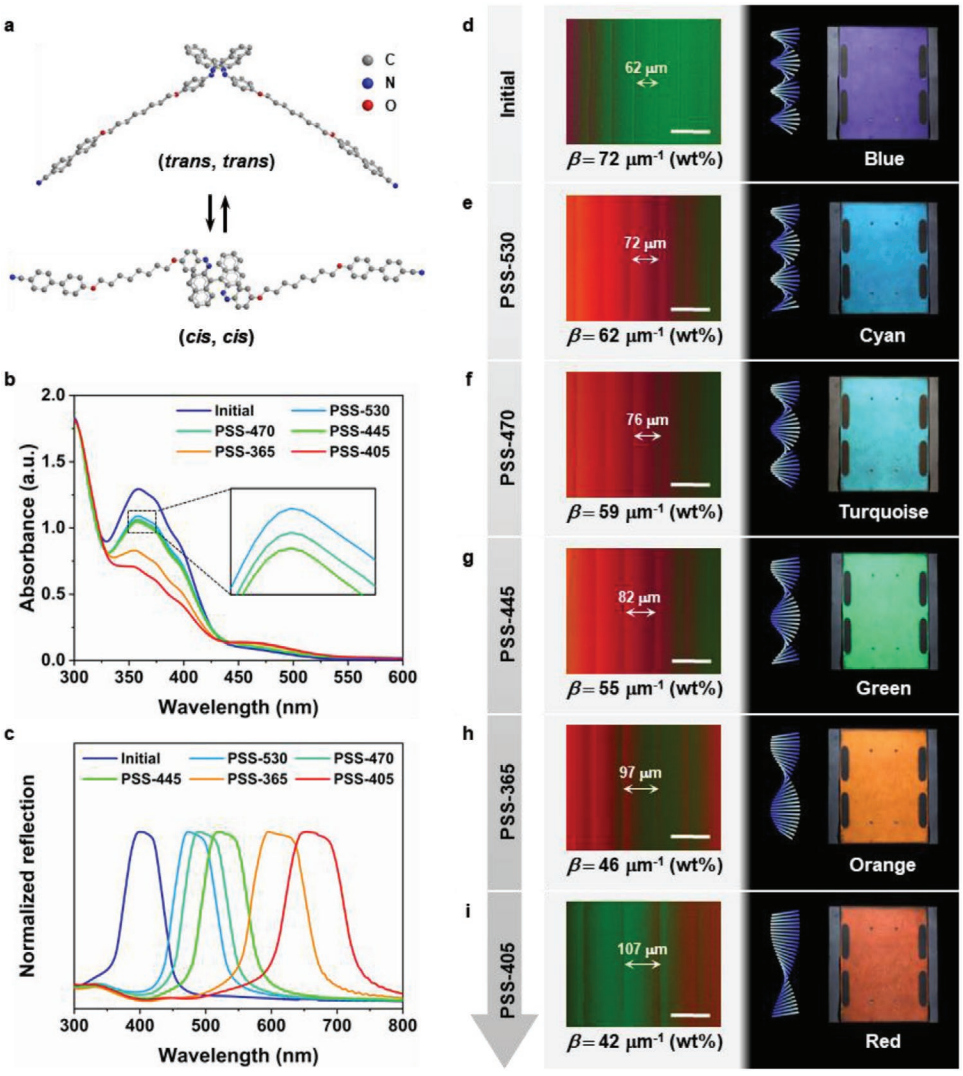

Figure 2. a) Schematic illustration to show the optimized molecular structures of (*trans*, *trans*) and (*cis*, *cis*) configurations of the photoresponsive chiral switch ABA. Hydrogen atoms are omitted for clarity. b) UV–vis spectra of ABA in CH_2Cl_2 ($c = 2 \times 10^{-5}$ M) at the initial state, PSS-530, PSS-470, PSS-445, PSS-365, and PSS-405. The inset plot (348–372 nm) shows the details of the π–π^* absorption peaks at the PSS-530, PSS-470, and PSS-445. c) Reflective spectra of the light-driven CLCs in a 15 μm thick antiparallel aligned cell at the initial state, PSS-530, PSS-470, PSS-445, PSS-365, and PSS-405. The light-driven CLCs contain 3.5 wt% ABA and 2.2 wt% S5011 in the LC host E7. d–i) Optical images to show the disclination lines of the CLC mixture containing 0.35 wt% ABA and 0.22 wt% S5011 in the LC host E7, and photographs to show blue, cyan, turquoise, green, orange, and red photostationary colors of the light-driven CLCs in a 15 μm thick antiparallel aligned cell (2.0 cm × 2.5 cm) at the initial state, PSS-530, PSS-470, PSS-445, PSS-365, and PSS-405, respectively. The light-driven CLCs contain 3.5 wt% ABA and 2.2 wt% S5011 in the LC host E7. The intensities of 530, 470, 445, 365, and 405 nm light are 20, 20, 30, 5, and 10 mW cm^{-2}. Irradiation times are all 30 s to reach the PSSs. Scale bar, 100 μm.

the "Experimental Section" and in Figure S8 (Supporting Information). A homogeneous mixture of monomers, crosslinkers, and light-driven CLCs was polymerized under UV light exposure to form the PDLC layer with uniform thickness controlled by polyester spacers (5 μm). As the polymeric chains grew in molecular weight, they were immiscible with the light-driven CLCs and generated polymer walls, which were testified by the morphology in the scanning electron microscope (SEM) image (Figure 3b).[46,47] Owing to the mobility of the LC molecules, the CLCs coalesced in microscale irregular droplets and were dispersed by the polymer walls (Figure S9, Supporting Information).[48] The polarized optical microscope (POM) image showing typical fan-shaped textures indicates that the CLC droplets confined in the PDLC layer are at the FC state (Figure 3c). Importantly, the resultant photonic paper was stored in darkness for *cis*–*trans* thermal relaxation of ABA since the UV light induced not only the polymerization but also the *trans*–*cis* isomerization during the fabrication.

The photonic paper capable of writing, tuning, and erasing was comprehensively investigated upon external stimuli, including pressure, light, and electricity (Figure 3d). At the initial state, the photonic paper exhibited a black appearance because the incident light was scattered forward by the randomly aligned helical axes at the FC state and was further absorbed by the bottom black PET.[40] The 0.8 mm wide sharp lines with blue color were written on the black background by

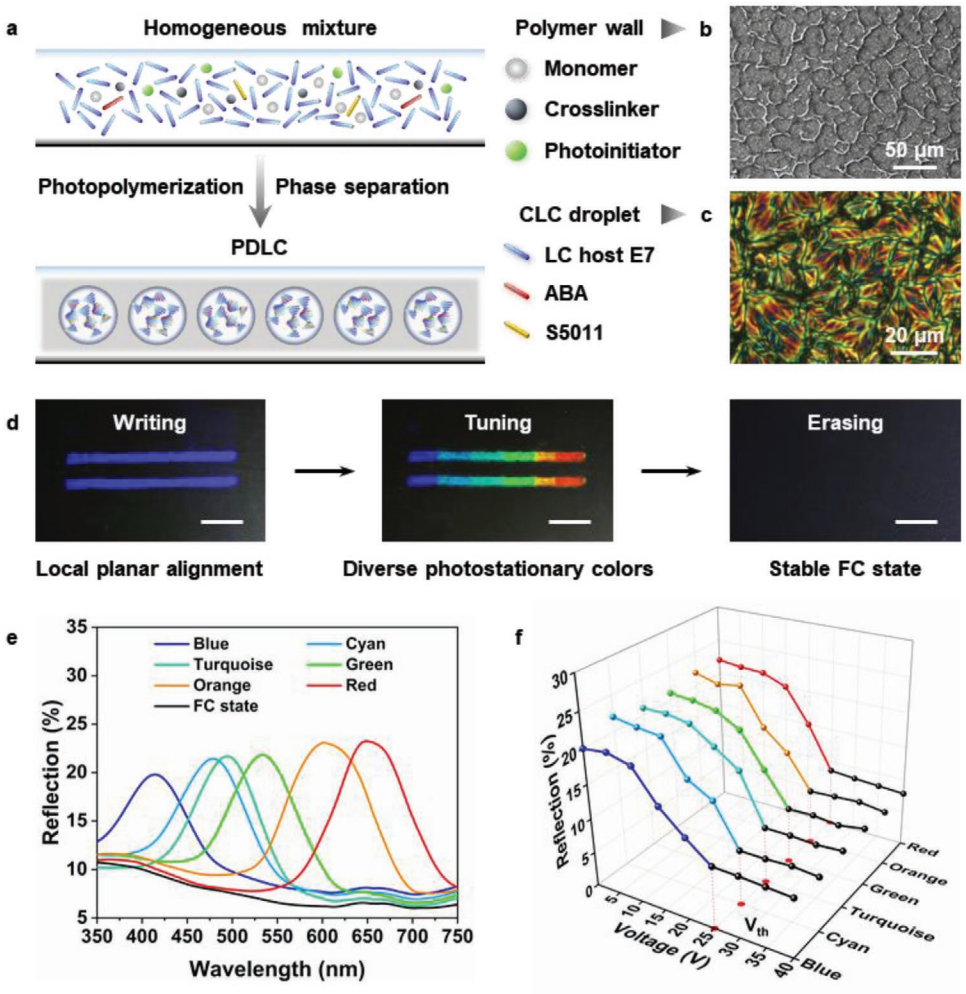

Figure 3. a) Schematic illustration to show the photopolymerization-induced phase separation of the homogeneous mixture. The microscale CLC droplets are confined by the polymer walls in the PDLC layer. b) A SEM image of the polymer walls in the PDLC layer (top view). c) A POM image of the FC state to show the typical fan-shaped textures in the CLC droplets. d) Photographs of the photonic paper to show writing, tuning, and erasing. The blue lines are written by a stylus, tuned to diverse photostationary colors by light of different wavelengths with a photomask, and erased by an electric field. Scale bar, 1 cm. e) Reflective spectra of the photonic paper at the FC state and planar states with different pitch lengths. f) Voltage–reflection curves of the photonic paper at the planar states with different pitch lengths. The threshold voltage (V_{th}) is 25 V to erase all the structural colors. The blue, cyan, turquoise, green, orange, and red colors are at the initial state, PSS-530, PSS-470, PSS-445, PSS-365, and PSS-405, respectively. The intensities of 530, 470, 445, 365, and 405 nm light are 20, 20, 30, 5, and 10 mW cm^{-2}, respectively. Irradiation times are all 30 s to reach the PSSs.

a stylus with a 1.0 mm wide tip (Figure S10, Supporting Information), originating from the locally pressure-induced reconfiguration from the FC to the planar state. The local planar alignment is attributed to two factors: flexible upper PET and polymer walls. Compared to the rigid glass cell that causes uniform distribution of the applied pressure, the flexible PET substrate concentrates the pressure on local areas via a slight change on thickness of the photonic paper (Figure S11, Supporting Information). Furthermore, the light-driven CLCs are restricted to microscale irregular droplets by the polymer walls in the PDLC layer, which limits the fluidity of the LC molecules upon pressure.[42] Such two factors result in the local planar alignment at the stress point where the scattering FC state is reconfigured to the reflecting planar state that exhibits structural colors. When the applied pressure is removed, the local planar alignment is stabilized by the anchoring effect of the polymer walls on LC molecules and has long-term stability for at least 20 days (Figure S12, Supporting Information).

Notably, the recorded blue lines were tuned to diverse photostationary colors with a photomask thanks to the phototunable pitch length of the light-driven CLCs. As the reflectance spectra are shown in Figure 3e, the central reflection wavelengths of blue, cyan, turquoise, green, orange, and red colors displayed on the photonic paper are consistent with those of the light-driven CLCs confined in the antiparallel aligned cell, indicating that introduction of the polymers into the CLC has a negligible effect on the photocontrol of the pitch length. The phototunable colors maintained for 20 min at ambient environment and eventually changed to green at the PSS under the room light (Figure S13, Supporting Information). When the photonic paper was stored in darkness, the phototunable colors gradually faded back to blue at the initial state within 12 h due

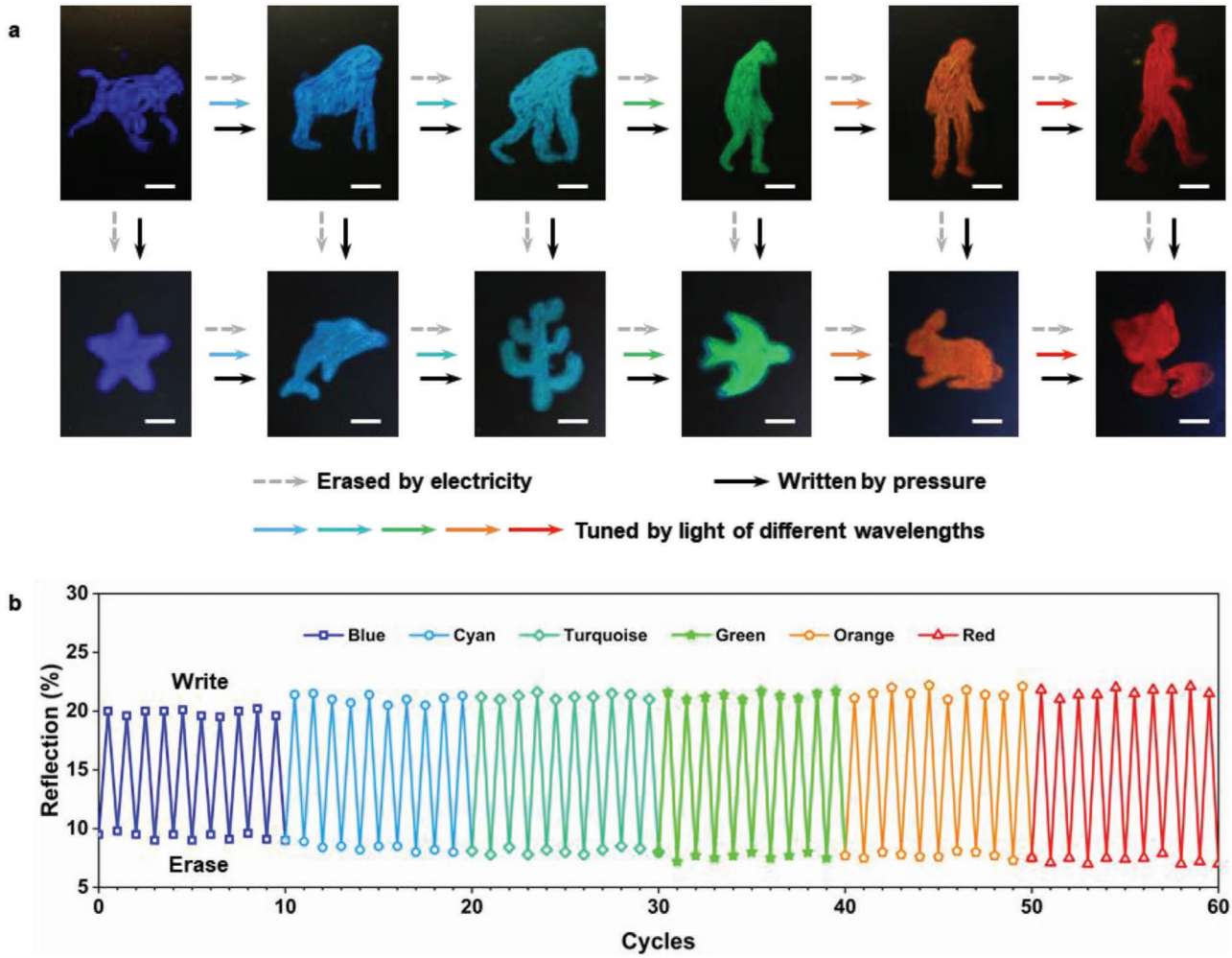

Figure 4. a) Photographs of the photonic paper to show the basic "write–erase" cycles of each single color (vertical direction) and the novel "tune–write–erase" mode of different photostationary colors (horizontal direction). The patterns are erased by a 25 V electric field (dashed gray arrows), tuned by light of different wavelengths (colorful arrows), and written by pressure (black arrows). The cyan, turquoise, green, orange, and red colors are tuned by 530, 470, 445, 365, and 405 nm light, respectively. Scale bar, 1 cm. b) A plot to show the variation in the reflectivity values at the different states upon repetitive writing, erasing, and tuning.

to the intrinsic thermal relaxation of the azobenzene photoswitches, and, however, could be quickly refreshed in a controllable manner upon exposure to light of different wavelengths (Figure S14, Supporting Information).

The threshold voltage for complete erasing was 25 V, which was measured via voltage–reflection curves of the photonic paper with different structural colors at the planar states (Figure 3f). Hence, in the presence of a 25 V alternating electric field (sine wave, 50 Hz), the multicolor lines were entirely erased since the planar state was switched to the FC state. Generally, the FC state tends to relax back to the planar state after the electric field is turned off. We note that the metastable FC state is stabilized by the enhanced anchoring effect on LC molecules rooted in irregularly porous microstructures of the polymer walls, and consequently remains stable even after removal of the electric field.[44]

Besides locally tuned after writing ("write–tune–erase"), the structural colors of the photonic paper are preset by light of different wavelengths before writing. As shown in **Figure 4**a, colorful patterns of human evolution are demonstrated stepwise according to the "tune–write–erase" mode (horizontal direction). A blue "*Pliopithecus*" pattern written on the photonic paper was first erased by the 25 V electric field because of the switching from the planar to FC state. The whole photonic paper was then exposed to 530 nm light that exerted photocontrol of the CLCs with the precise pitch length at the PSS-530 (cyan), whereas the helical axes remained unchanged at the FC state exhibiting black appearance. In this scenario, a cyan "*Dryopithecus*" pattern was drawn with the stylus by pressure-induced reconfiguration from the FC to planar state. Repeating these operations and changing the wavelengths of the light stimuli, we demonstrated colorful patterns of turquoise "*Australopithecus*," green "*Homo habilis*," orange "*Homo erectus*," and red "*Homo sapiens*" in sequence (Movie S2, Supporting Information). Different patterns of the same color were also rewritten and erased in term of basic "write–erase" cycles

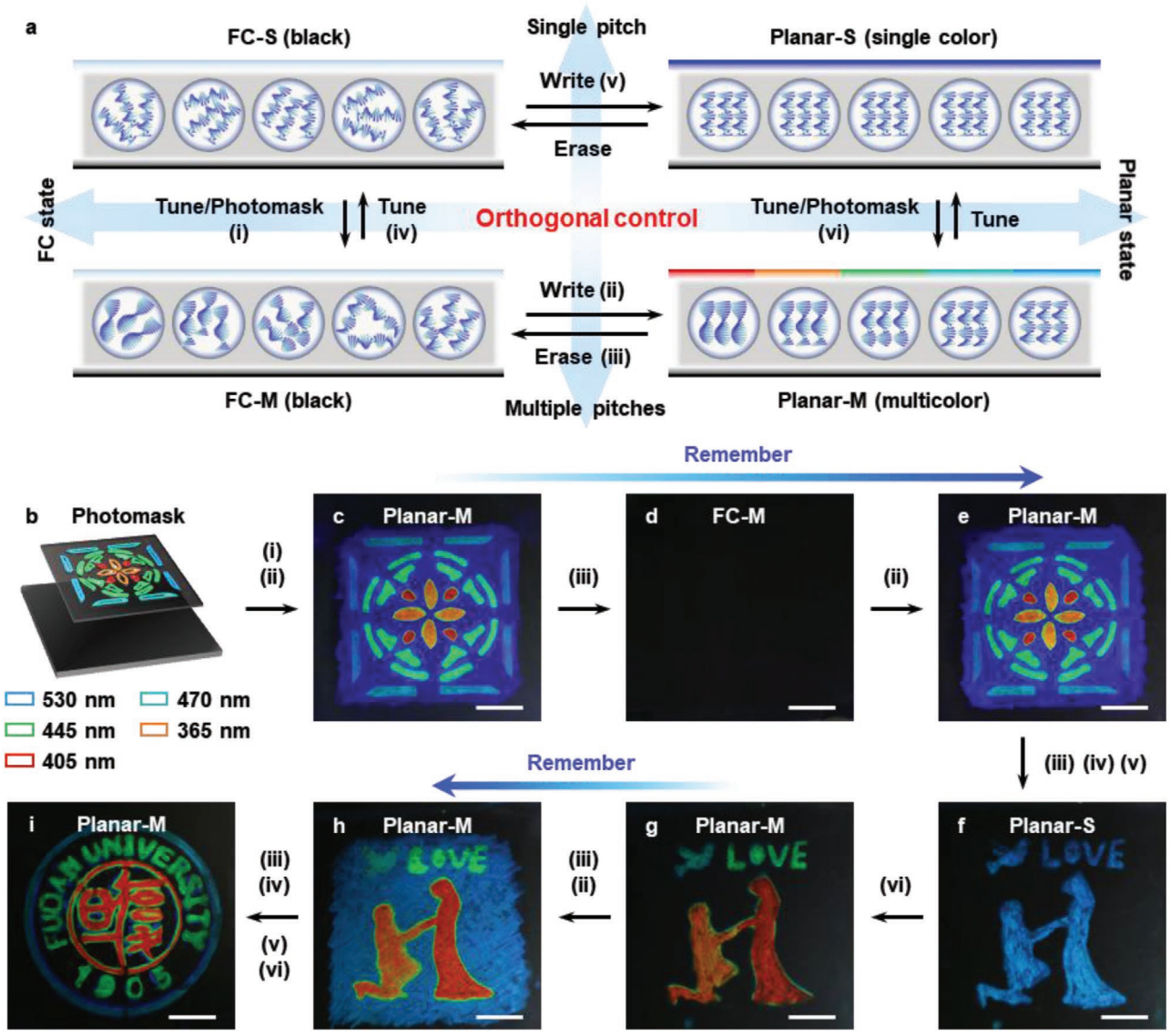

Figure 5. a) Schematic illustration to show the orthogonal control of the optical states (helical axis) and structural colors (pitch) in the photonic paper. Both the FC state of single pitch (FC-S) and the FC state of multiple pitches (FC-M) exhibit black appearance. The planar state of single pitch (Planar-S) exhibits single-color patterns. The planar state of multiple pitches (Planar-M) exhibits multicolor patterns. b) Schematic illustration to show the localized color tuning before writing via the photomask with a pattern of Chinese paper cutting. The colors of the rectangles represent the resultant photostationary colors tuned by light of different wavelengths. c–i) Sequential photographs to show the distinct multicolor patterns recorded on the photonic paper by optically tuning, mechanically writing, and electrically erasing. The blue arrows denote the process of "color memory effect" to remember the latest optically addressed images. Steps (i)–(vi) are the operations depicted in panel (a). Scale bar, 1 cm.

by alternating stimulation of pressure and electric field (vertical direction). Moreover, multicolor lines were directly written on the photonic paper, which was divided into several areas preset to different photostationary colors (Movie S3, Supporting Information). The photonic paper remained stable reflectivity of each color (blue, cyan, turquoise, green, orange, and red) at the reflecting planar and scattering FC states after 60 cycles (10 cycles for each color), suggesting acceptable fatigue resistance (Figure 4b).

Encouraged by orthogonal manipulation of the structural colors (pitch) and optical states (helical axis), we create intricate multicolor patterns on the photonic paper and further demonstrate the proof of concept for color memory. As **Figure 5**a shows, the self-organized helical superstructures of the light-driven CLCs in the PDLC layer are flexibly programmed among four conditions. The FC states of both single pitch length (FC-S) and multiple pitch lengths (FC-M) exhibit black appearance, while the planar states of single pitch length (Planar-S) and multiple pitch lengths (Planar-M) display single-color and multicolor patterns, respectively. First, by using the photomask with a pattern of Chinese paper cutting, the photonic paper is tuned from the FC-S to FC-M state upon localized exposure to light of different wavelengths (Figure 5b, step i). The optically "stamped" pattern is displayed by applying

pressure that induces the Planar-M state of the photonic paper (Figure 5c, step ii). The size of the resultant multicolor pattern tuned by light is the same as that of the photomask (Figure S15, Supporting Information). With the application of the 25 V electric field, the multicolor pattern of Chinese paper cutting is entirely erased, and the photonic paper transforms to the FC-M state (Figure 5d, step iii).

It is worth noting that the erased multicolor pattern of Chinese paper cutting is intactly restored on the photonic paper by applying pressure again (Figure 5e, step ii), which reveals that our photonic paper can remember the latest optically addressed patterns (color memory effect). The switching of the helical axes between the planar and FC states is independently manipulated by pressure and electricity without altering the phototunable pitch lengths of the CLC, and vice versa. Although the helical axes are switched from the planar to FC state by the electric field, the multiple pitch lengths triggered by localized light irradiation remain the same. Next, the multicolor pattern of Chinese paper cutting is changed to a single cyan pattern of romantic marriage proposal at the Planar-S state via erasing, tuning, and rewriting (Figure 5f, steps iii–v). The colors of the woman, man, LOVE, and pigeon are further tuned to red, orange, green, and turquoise for generating the multicolor pattern (Figure 5g, step vi), which is hidden with the application of the electric field and is also remembered by applying pressure (Figure 5h, steps ii and iii; Movie S4, Supporting Information). Furthermore, any multicolor patterns can be repeatedly recorded on our photonic paper after facile operations that manipulate the pitch lengths or helical axes (Figure 5i, steps iii–vi), showing the ability to transfer extensive information by mechanically writing, optically localized tuning, and the electrically erasing structural colors of the responsive photonic crystals.

3. Conclusion

In summary, we reported a novel strategy to write, erase, and importantly to tune the structural colors of the rewritable photonic paper by orthogonally manipulating the reconfigurable helical axes and phototunable pitch lengths of the self-organized helical superstructures. The light-driven CLCs with diverse photostationary colors were induced by the binary chiral system consisting of the newly designed ABA and S5011, which determined appropriate HTP values and endowed the CLC with the exact pitch lengths. Furthermore, the resultant CLC sandwiched by two flexible PET substrates was dispersed in the PDLC layer via photopolymerization-induced phase separation to fabricate the photonic paper. Compared to the traditional PDLCs that only exhibit patterns of static and fixed colors, our PDLC containing light-driven CLCs enables precisely dynamic phototuning of the colors in patterns. Therefore, according to the new working principle, any multicolor patterns are clearly written upon pressure, locally tuned by light of different wavelengths, and completely erased with the application of the electric field in a programmable manner. The basic "write–erase" cycles are promoted to "tune–write–erase" and "write–tune–erase" modes via employment of additional color tuning before or after writing. Interestingly, the optically "stamped" patterns could be hidden and restored due to the "color memory effect" provided by orthogonal manipulation of the two structural elements (reconfiguration and lattice constant), which develops a new concept for multistimuli-driven modulation of the periodic structures in responsive photonic crystals. This inkless photonic paper has enormous potential to improve the user experience, opening an avenue to record, program, and remember intricate images in visualized color information and user-interactive display technologies.

4. Experimental Section

Synthesis of the photoresponsive chiral switch ABA and measurement of the HTP values are described in the Supporting Information.

Materials: All chemicals and solvents were purchased from commercial suppliers and used without further purification. Deuterated solvents were purchased from Cambridge Isotope Laboratory. The LC host E7 ($\Delta n = 0.223$, $\Delta\varepsilon > 0$, $M = 271.74$ g mol^{-1}), standard chiral dopants S5011 and R5011 were purchased from Nanjing Murun Advanced Material Co., Ltd. Wedge cells (KCRK-07) and antiparallel aligned cells were purchased from EHC Co., Ltd. Poly(ethylene glycol) methacrylates (PEGMA, M_n = 500 g mol^{-1}), 2-hydroxyethyl methacrylates (HEMA), poly(ethylene glycol) diacrylates (PEGDA, M_n = 250 g mol^{-1}), and photoinitiator IRG651 were purchased from Shanghai Taitan Scientific Co., Ltd. The transparent colorless PET films (thickness: 125 µm) coated with ITO and black PET films (thickness: 188 µm) coated with ITO were purchased from Zhuhai Singyes New Materials Technology Co., Ltd. Polyester spacers (5 µm) were purchased from Suzhou Nanomicro Technology Co., Ltd.

Preparation of the Light-Driven CLC Mixtures: 3.5 wt% photoresponsive chiral switch ABA, 2.2 wt% chiral dopant S5011, and LC host E7 were dissolved in dichloromethane solution. After evaporation of the solvent in an oven at 50 °C, the mixture was stored in darkness for 12 h.

Fabrication of the Rewritable Photonic Paper: First, 44.55 wt% PEGMA, 4.95 wt% HEMA, 49.5 wt% PEGDA, and 1.0 wt% photoinitiator IRG651 were mixed to form a homogeneous polymerizable liquid. Second, a mixture of 15.0 wt% polymerizable liquid, 85 wt% light-driven CLC, and polyester spacers (5 µm) was sandwiched between a transparent colorless ITO-coated PET film and a black ITO-coated PET film, and subsequently was evenly spread out by the rolling process. Third, polymerization of the mixture was induced by UV irradiation (365 nm, 15 mW cm^{-2}) for 50 min to form the PDLC layer. Last, the rewritable paper was stored in darkness for 12 h to restore ABA back to the (*trans*, *trans*) form before used.

Supporting Information

Supporting Information is available from the Wiley Online Library or from the author.

Acknowledgements

S.C. and L.Q. contributed equally to this work. This work was financially supported by the National Natural Science Foundation of China (Grant Nos. 51903053 and 51721002), National Key R&D Program of China (Program No. 2017YFA0701302), and Natural Science Foundation of Shanghai (Grant No. 21ZR1405900).

Conflict of Interest

The authors declare no conflict of interest.

Data Availability Statement

The data that support the findings of this study are available from the corresponding author upon reasonable request.

Keywords

cholesteric liquid crystals, photoresponsive chiral switches, polymer dispersed liquid crystals, rewritable paper, tunable structural colors

Received: October 1, 2021
Revised: November 29, 2021
Published online:

[1] M. I. Khazi, W. Jeong, J.-M. Kim, *Adv. Mater.* **2018**, *30*, 1705310.
[2] Y. Fang, Y. Ni, S.-Y. Leo, C. Taylor, V. Basile, P. Jiang, *Nat. Commun.* **2015**, *6*, 7416.
[3] W. Jeong, M. I. Khazi, D.-H. Park, Y.-S. Jung, J.-M. Kim, *Adv. Funct. Mater.* **2016**, *26*, 5230.
[4] G. Xi, L. Sheng, J. Du, J. Zhang, M. Li, H. Wang, Y. Ma, S. X.-A. Zhang, *Nat. Commun.* **2018**, *9*, 4819.
[5] Z. Wang, D. Xie, F. Zhang, J. Yu, X. Chen, C. P. Wong, *Sci. Adv.* **2020**, *6*, eabc2181.
[6] P. Zhang, G. Zhou, L. T. de Haan, A. P. H. J. Schenning, *Adv. Funct. Mater.* **2021**, *31*, 2007887.
[7] J. Du, L. Sheng, Y. Xu, Q. Chen, C. Gu, M. Li, S. X.-A. Zhang, *Adv. Mater.* **2021**, *33*, 2008055.
[8] J. Ge, Y. Yin, *Angew. Chem., Int. Ed.* **2011**, *50*, 1492.
[9] K. Chen, Q. Fu, S. Ye, J. Ge, *Adv. Funct. Mater.* **2017**, *27*, 1702825.
[10] L. Shang, W. Zhang, K. Xu, Y. Zhao, *Mater. Horiz.* **2019**, *6*, 945.
[11] Y. Wang, L. Shang, G. Chen, L. Sun, X. Zhang, Y. Zhao, *Sci. Adv.* **2020**, *6*, eaax8258.
[12] Y. Yang, Y. Chen, Z. Hou, F. Li, M. Xu, Y. Liu, D. Tian, L. Zhang, J. Xu, J. Zhu, *ACS Nano* **2020**, *14*, 16057.
[13] H. Fudouzi, Y. Xia, *Adv. Mater.* **2003**, *15*, 892.
[14] J. Ge, J. Goebl, L. He, Z. Lu, Y. Yin, *Adv. Mater.* **2009**, *21*, 4259.
[15] S. Yu, X. Cao, W. Niu, S. Wu, W. Ma, S. Zhang, *ACS Appl. Mater. Interfaces* **2019**, *11*, 22777.
[16] H. Wan, X. Li, L. Zhang, X. Li, P. Liu, Z. Jiang, Z.-Z. Yu, *ACS Appl. Mater. Interfaces* **2018**, *10*, 5918.
[17] R. Chen, D. Feng, G. Chen, X. Chen, W. Hong, *Adv. Funct. Mater.* **2021**, *31*, 2009916.
[18] H. S. Kang, J. Lee, S. M. Cho, T. H. Park, M. J. Kim, C. Park, S. W. Lee, K. L. Kim, D. Y. Ryu, J. Huh, E. L. Thomas, C. Park, *Adv. Mater.* **2017**, *29*, 1700084.
[19] H. Fudouzi, Y. Xia, *Langmuir* **2003**, *19*, 9653.
[20] Y. Xie, Y. Meng, W. Wang, E. Zhang, J. Leng, Q. Pei, *Adv. Funct. Mater.* **2018**, *28*, 1802430.
[21] Y. Wang, Q. Zhao, X. Du, *Mater. Horiz.* **2020**, *7*, 1341.
[22] J. Hou, M. Li, Y. Song, *Angew. Chem., Int. Ed.* **2018**, *57*, 2544.
[23] S. Liu, Y. Yang, L. Zhang, J. Xu, J. Zhu, *J. Mater. Chem. C* **2020**, *8*, 16633.
[24] H. S. Kang, S. W. Han, C. Park, S. W. Lee, H. Eoh, J. Baek, D.-G. Shin, T. H. Park, J. Huh, H. Lee, D.-E. Kim, D. Y. Ryu, E. L. Thomas, W.-G. Koh, C. Park, *Sci. Adv.* **2020**, *6*, eabb5769.
[25] K. Szendrei, P. Ganter, O. Sànchez-Sobrado, R. Eger, A. Kuhn, B. V. Lotsch, *Adv. Mater.* **2015**, *27*, 6341.
[26] Y. Kim, N. Tamaoki, *ChemPhotoChem* **2019**, *3*, 284.
[27] Z. Zheng, Y. Li, H. K. Bisoyi, L. Wang, T. J. Bunning, Q. Li, *Nature* **2016**, *531*, 352.
[28] S. Han, Y. Chen, B. Xu, J. Wei, Y. Yu, *Chin. J. Polym. Sci.* **2020**, *38*, 806.
[29] H. K. Bisoyi, Q. Li, *Chem. Rev.* **2016**, *116*, 15089.
[30] X. Liu, L. Qin, Y. Zhan, M. Chen, Y. Yu, *Acta Chim. Sin.* **2020**, *78*, 478.
[31] L. Wang, A. M. Urbas, Q. Li, *Adv. Mater.* **2020**, *32*, 1801335.
[32] L. Qin, X. Liu, K. He, G. Yu, H. Yuan, M. Xu, F. Li, Y. Yu, *Nat. Commun.* **2021**, *12*, 699.
[33] H. K. Bisoyi, Q. Li, *Acc. Chem. Res.* **2014**, *47*, 3184.
[34] A. Ryabchun, F. Lancia, J. Chen, D. Morozov, B. L. Feringa, N. Katsonis, *Adv. Mater.* **2020**, *32*, 2004420.
[35] R. A. van Delden, N. Koumura, N. Harada, B. L. Feringa, *Proc. Natl. Acad. Sci. USA* **2002**, *99*, 4945.
[36] Q. Li, L. Green, N. Venkataraman, I. Shiyanovskaya, A. Khan, A. Urbas, J. W. Doane, *J. Am. Chem. Soc.* **2007**, *129*, 12908.
[37] T. J. White, R. L. Bricker, L. V. Natarajan, N. V. Tabiryan, L. Green, Q. Li, T. J. Bunning, *Adv. Funct. Mater.* **2009**, *19*, 3484.
[38] L. Qin, W. Gu, J. Wei, Y. Yu, *Adv. Mater.* **2018**, *30*, 1704941.
[39] Q. Li, Y. Li, J. Ma, D.-K. Yang, T. J. White, T. J. Bunning, *Adv. Mater.* **2011**, *23*, 5069.
[40] D.-K. Yang, *J. Disp. Technol.* **2006**, *2*, 32.
[41] L. Qin, J. Wei, Y. Yu, *Adv. Opt. Mater.* **2019**, *7*, 1900430.
[42] H. Xing, X. Wang, J. Xu, J. Wei, J. Guo, *RSC Adv.* **2013**, *3*, 17822.
[43] P. Chen, L.-L. Ma, W. Hu, Z.-X. Shen, H. K. Bisoyi, S.-B. Wu, S.-J. Ge, Q. Li, Y.-Q. Lu, *Nat. Commun.* **2019**, *10*, 2518.
[44] D.-K. Yang, J. L. West, L.-C. Chien, J. W. Doane, *J. Appl. Phys.* **1994**, *76*, 1331.
[45] X. Liang, S. Guo, M. Chen, C. Li, Q. Wang, C. Zou, C. Zhang, L. Zhang, S. Guo, H. Yang, *Mater. Horiz.* **2017**, *4*, 878.
[46] D.-K. Yang, X.-Y. Huang, Y.-M. Zhu, *Annu. Rev. Mater. Sci.* **1997**, *27*, 117.
[47] E. Montbach, D. J. Davis, A. Khan, T. Schneider, D. Marhefka, O. Pishnyak, T. Ernst, N. Miller, J. W. Doane, *Proc. SPIE* **2009**, *7232*, 723203.
[48] H. Wang, L. Wang, M. Chen, T. Li, H. Cao, D.-K. Yang, Z. Yang, H. Yang, S. Zhu, *RSC Adv.* **2015**, *5*, 58959.